

From transient localization to band transport: on quantum corrections and lack thereof

S. Fratini¹, S. Ciuchi²

¹*Université Grenoble Alpes, CNRS, Grenoble INP,
Institut Néel, 38000 Grenoble, France*

²*Dipartimento di Scienze Fisiche e Chimiche
Università dell'Aquila, via Vetoio,
I-67010 Coppito-L'Aquila, Italy*

(Dated: April 1, 2019)

Transient localization has emerged as a powerful theoretical framework that is able to describe charge transport in high-mobility organic semiconductors, where the carrier diffusion is strongly limited by their coupling to thermal molecular motions. As continuous efforts are devoted to suppressing the localization effects ensuing from such dynamic disorder, it can be expected that future organic compounds will progressively move closer to the band transport regime. We devise here a unified theoretical framework that encompasses both transient localization and Bloch-Boltzmann transport theory, bridging the gap between these two limiting descriptions. This allows us to precisely assess the conditions required for localization corrections to become negligible, and enables a proper description of materials in the intermediate crossover regime.

Introduction. The last decade has witnessed considerable progress in the understanding of charge transport in high-mobility organic semiconductors, with important milestones achieved in both experimental and theoretical research. On the experimental side, the widespread access and improved control on field-effect devices has provided a common ground for the systematic and reproducible measurement of carrier mobilities [1]. Initially restricted to crystalline rubrene [2, 3], which served as a prototypical material due to its outstanding performances and stability, results indicative of intrinsic charge transport are now obtained in a growing number of organic semiconductors [4–10]. On the theoretical side, it is now understood that the intrinsic factor limiting the mobility in these materials is the presence of large thermal vibrations of the constituent molecules. These cause strong dynamic disorder, which hinders the carrier motion in ways that differ substantially from what predicted for electrons weakly scattered by phonons. The physical idea of charge carriers being transiently localized by dynamic molecular disorder is now supported by a whole body of theory, relying on extensive numerical evidence, analytical developments and experimental validations [11].

Building on these achievements, the field is now jointly aiming at devising and synthesizing compounds equalling, or even surpassing, the performances of rubrene [10, 12–14]. If the desired improvements in mobility are indeed realized, future compounds and devices could move to a regime of transport where localization effects become less relevant, progressively approaching the band transport regime. In order to address this foreseeable situation, we establish here a theory of transport that encompasses both the transient localization scenario relevant when dynamic disorder is strong, and Bloch-Boltzmann band theory that applies to more con-

ventional phonon and weak disorder scattering, spanning the whole region comprised between these two limits.

A general theory of transport. Our derivation builds on the Kubo response formalism as presented in Refs. [15, 16]. The key quantity of interest is the time-dependent velocity-velocity anticommutator correlation function, $C(t) = \langle \{\hat{V}(t), \hat{V}(0)\} \rangle$, with \hat{V} the velocity operator for charge carriers in a given direction. Denoting as $C_{SC}(t)$ the correlator obtained from semiclassical transport theory, we define as *quantum localization corrections* the quantity $\delta C = C - C_{SC}$, describing all those velocity correlations that are not included in the semiclassical description [17]. Such corrections, which entail the quantum nature of the electronic wavefunctions, can be determined exactly in the limit of static disorder: numerical diagonalization of the one-body disordered Hamiltonian in this case yields the full correlator, $C_0(t)$ (the index 0 stands for frozen disorder). The semiclassical part can also be calculated for the same Hamiltonian by standard methods [19]. Combining these two quantities gives full access to δC in the frozen disorder limit.

Dynamic motion of the scattering centers destroys the quantum interferences at the very origin of wavefunction localization [17, 18]. As a result, localization effects are only sustained at times shorter than the timescale of disorder dynamics, τ_{in} , while they are suppressed at longer times, enabling carrier diffusion. In the relaxation time approximation as originally formulated in Refs. [15, 20], this behavior was modeled by assuming an exponential decay of the current correlations, $C(t) = C_0(t)e^{-t/\tau_{in}}$. From this simple form, the full body of transient localization (TL) theory was derived, revealing a direct relationship between the mobility of the carriers and their localization properties [15].

We propose here the following generalization,

$$C(t) = C_{SC}(t) + [C_0(t) - C_{SC}(t)]e^{-t/\tau_{in}}, \quad (1)$$

where the relaxation is properly applied not to the full correlator, but to the localization corrections only. Contrary to the original formulation, Eq. (1) is now fully consistent with the underlying physical idea of decaying localization corrections. This new form brings both quantitative and conceptual improvements, as it now explicitly interpolates between full localization and semiclassical transport, which are obtained respectively in the limits $\tau_{in} \rightarrow \infty$ and $\tau_{in} \rightarrow 0$. Moreover, it follows from Eq. (1) that if localization corrections are negligible to start with, the term between brackets can be dropped, recovering the semiclassical result regardless of the value of τ_{in} . On the other hand, when localization effects are present, these will dominate C_0 at long times. In this case we can safely set $C_{SC}(t) = 0$ in Eq. (1), fully recovering transient localization theory.

The instantaneous diffusivity of the charge carriers is obtained as $D(t) = \int_0^t C(t')dt'/2$ [15]. Applying the Laplace transform $\tilde{C}(p) = \int_0^\infty C(t)e^{-pt}dt$ to Eq. (1), with $p = 1/\tau_{in}$, yields the diffusion constant $\mathcal{D} = \lim_{t \rightarrow \infty} D(t) = [\tilde{C}_{SC}(0) + \tilde{C}_0(p) - \tilde{C}_{SC}(p)]/2$. The mobility is finally obtained using Einstein's relation:

$$\mu = \frac{e}{k_B T} \frac{pL^2(p)}{2} + \frac{e}{2k_B T} [\tilde{C}_{SC}(0) - \tilde{C}_{SC}(p)]. \quad (2)$$

The first term is the usual TL result [15], which dominates at small p (large τ_{in}), where $L^2(p) = \tilde{C}_0(p)/p$ defines the squared transient localization length. Using the expression $\mathcal{D}_{SC} = \tilde{C}_{SC}(0)/2$ for the semiclassical diffusion constant, the first term between brackets is easily recognized as the band mobility.

Model and method. We now apply the theory to the ensemble of tight-binding models introduced in Ref. [12], representative of a wide class of high-mobility molecular semiconductors. These are defined by charge carriers moving on a hexagonal molecular lattice of unit spacing a , with nearest neighbor transfer integrals J_i in the different bond directions $i = a, b, c$ (see the sketch in Fig. 1). The J_i are dynamically modulated by thermal inter-molecular motions of frequency p , leading to gaussian fluctuations of spread ΔJ_i , that we take to be uncorrelated between different bonds. The parameters $J = \sqrt{J_a^2 + J_b^2 + J_c^2}$ and $\Delta J = \sqrt{\Delta J_a^2 + \Delta J_b^2 + \Delta J_c^2}$ set the scale of the electronic dispersion and of the overall energetic disorder respectively.

To implement Eq. (1) we calculate the current-current correlation function C_0 of the frozen disorder limit via numerical solution of the one-body tight-binding hamiltonian with gaussianly distributed J_i s, using alternatively the quantum diffusion method of Ref. 12 or direct diagonalization as described in Ref. 21. For the semiclassical part we use instead the standard Bloch-Boltzmann band

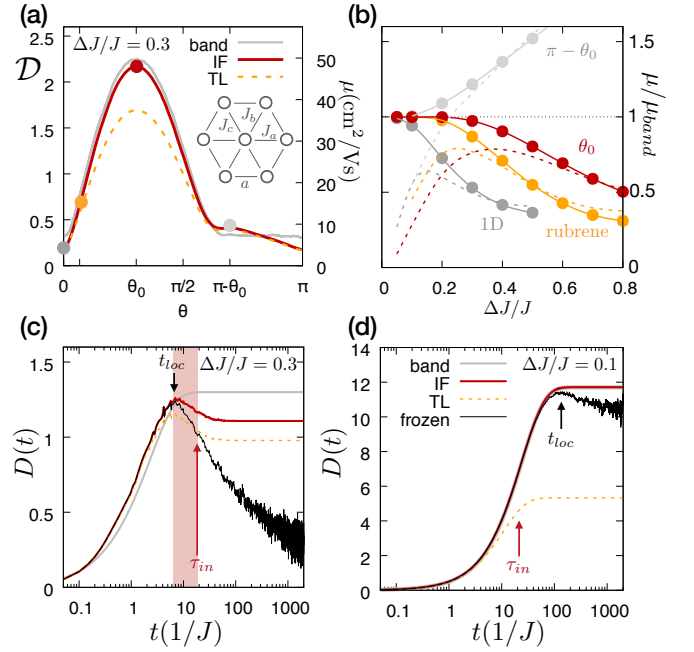


FIG. 1: (a) Diffusion constant of hole carriers on the tight-binding model defined in the text, averaged over the two perpendicular directions as a function of θ , for $\Delta J/J = 0.3$ and $T/J = 0.25$: band theory (band), the interpolation formula Eq. (2) (IF) and transient localization theory (TL). The angle $\theta_0 = \arccos(1/\sqrt{3})$ corresponds to the isotropic point $J_a = J_b = J_c$. Diffusion is in units of $a^2 J/\hbar$, the right axis is the corresponding mobility using $a = 6\text{\AA}$. The sketch represents the hexagonal lattice used in this work. (b) Mobility scaled w.r.t. the band result, as a function of disorder strength, for the structures indicated by the labels, corresponding to $\theta = 0, 0.21, \theta_0$ and $\pi - \theta_0$ (see also symbols in panel a): TL (dashed lines) and IF (full lines and symbols). (c) Time-dependent diffusivity calculated in the direction of highest mobility for the band structure of rubrene, $\theta = 0.21$, with $\Delta J/J = 0.3$ and $\tau_{in} = 20/J$. Time is in units of $1/J$. The arrows and shaded area indicate the *transient localization* time (see text). (d) same, with $\Delta J/J = 0.1$.

theory result [19], as described in Ref. [12]. Unless otherwise specified, we take J as the energy unit and set $\hbar = 1$ in the following.

Results. Fig. 1 illustrates how the theory performs across the ensemble of band structures spanned by our two-dimensional model. We focus for clarity on the common situation where two bond directions are equal by symmetry, so that the set of transfer integrals can be characterized by a single parameter θ ($J_a = J \cos \theta$, $J_b = J_c = J \sin \theta/\sqrt{2}$). How different crystals are affected by disorder is directly reflected in the TL diffusion constant [12], which is directly proportional to the square of the transient localization length, $\mathcal{D}_{TL} = pL^2(p)/2$ (Fig. 1a, orange dashed). In all those cases where localization effects are strong (one-dimensional lattices, $\theta = 0, \pi$, and all structures around $\pi - \theta_0$, yielding low

diffusion constants), the correction term in Eq. (2) appears to be negligible at the chosen value of energetic disorder, $\Delta J/J = 0.3$, and the interpolating theory (red) essentially coincides with the TL value. The interpolating theory instead markedly deviates from the TL result upon moving towards the isotropic point, $\theta = \theta_0$, actually coming very close to the semiclassical value (gray).

The interpolating nature of Eq. (2) is best seen in Fig. 1b, where we show the ratio μ/μ_{band} of the calculated mobility to the semiclassical prediction, for selected structures. The latter is given by $\mu_{band} \propto (\Delta J/J)^{-\gamma}$, with an exponent $\gamma = 2$ reflecting second order scattering processes [12]. By construction, TL theory (dashed lines) applies when localization effects are so strong that they set in within the timescale τ_{in} of molecular motions [15, 16, 22]. In this regime, localization processes lead to mobilities that are generally lower than the band value by up to a factor of three [23]. Localization processes also lead to a steeper dependence on disorder, with power law exponents reaching as high as $\gamma = 3.4$ for rubrene and $\gamma = 3.2$ in the isotropic case at large disorder. The structures around $\pi - \theta_0$ are exceptions, exhibiting an opposite behavior: there, due to a negative combination of the signs of the transfer integrals, $J_a J_b J_c < 0$, a van Hove singularity of states with anti-localization properties arises close to the hole band edge. Thermal population of these states causes the mobility to rise above the band value; the mobility is still a decreasing function of disorder, but with a reduced exponent as low as $\gamma = 1.5$.

The breakdown of TL theory upon reducing the disorder strength is directly reflected in Fig. 1b, as the ratio μ/μ_{band} incorrectly goes through a maximum, marking the crossover to semiclassical behavior (see below). The interpolation formula Eq. (2) corrects this drawback, interpolating smoothly from the TL result at strong disorder to the expected Boltzmann limit at weak disorder (full curves and symbols).

The crossover to semiclassical transport can be understood by tracking the time-dependent diffusivity as shown in Fig. 1c. As a representative choice of parameters, we take the band structure of rubrene and set the energetic disorder to $\Delta J/J = 0.3$ [12]. The diffusivity of the system with frozen molecular displacements, $D_0(t)$, is shown for reference (black thin line). Here, localization processes are responsible for the decrease of the diffusivity at long times, and its vanishing as $t \rightarrow \infty$. The onset of localization, t_{loc} , can therefore be identified with the locus of the maximum of $D_0(t)$. By contrast, such a maximum and subsequent decrease is absent in the semiclassical diffusivity, which does not contain localization corrections (gray). In TL theory (orange dashed), the assumed exponential relaxation of current correlations freezes the long-time decay of $D_0(t)$ at the characteristic time of molecular fluctuations, hence yielding a finite diffusion constant $\mathcal{D}_{TL} \sim D_0(\tau_{in})$. It is precisely the existence of a time lag between t_{loc} and the recov-

ery of diffusion at τ_{in} that defines *transient localization* (shaded), causing the diffusion constant to deviate from the band value. In the example shown, the diffusivity of the interpolating theory (red) is qualitatively similar to the TL result.

Reducing the disorder strength or, analogously, moving to more isotropic structures, suppresses localization effects. This is reflected in a longer onset time t_{loc} and consequently larger diffusivities, as shown in Fig. 1d for $\Delta J/J = 0.1$. Following the argument given above, localization corrections are totally washed out when t_{loc} attains τ_{in} , as in that case they do not have time to develop, being cut off at their very onset. The condition $t_{loc} \sim \tau_{in}$ therefore marks the crossover to semiclassical behavior. Beyond that point, TL theory would provide an incorrect (under)estimate of the diffusion constant (dashed line in Fig. 1d), which explains the non-monotonic behavior exhibited in Fig. 1b. The correct low-disorder limit is instead recovered by the interpolation theory, which in this regime becomes indistinguishable from the semiclassical result (red and gray curves in Fig. 1d).

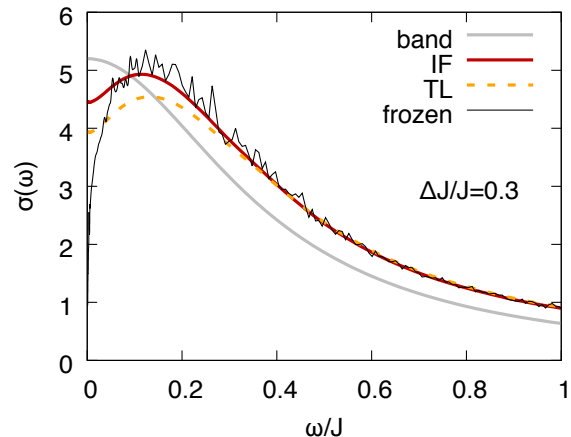


FIG. 2: Optical conductivity per particle, corresponding to the time-dependent diffusivities shown in Fig. 1c (microscopic parameters of rubrene).

Optical conductivity and semiclassical crossover. In the band limit, the optical conductivity per particle exhibits a simple Lorentzian (Drude) shape whose width is set by the semiclassical scattering rate $1/\tau$, $\sigma_{band}(\omega) = e\mu_{band}/(1 + \omega^2\tau^2)$ (gray line in Fig. 2), with $\mu_{band} = e\tau/m^*$ and m^* the band mass [19]. Localization processes induce a shift of the absorption maximum to finite frequencies [15, 22, 24], which is captured both in the TL and in the interpolating theory (orange dashed and red full line respectively). Interestingly, the standard band theory approach fails to reproduce the correct behavior at high frequencies $\omega \gg 1/\tau$, where the frozen disorder limit is known to be accurate (black thin line) [25]. The correct high-frequency absorption is instead properly recovered by both the TL theory and the IF.

The emergence of a dip at $\omega = 0$ is a precursor to the full suppression of the d.c. conductivity expected in the localized limit [22, 25, 26], and it is therefore a direct signature of the breakdown of band transport. It can be conveniently tracked from the change of curvature of $\sigma(\omega)$ at $\omega = 0$, which provides us with a rigorous criterion to locate the crossover between the TL and band regime. To this aim we take advantage of the exact formula that was derived in Ref. 15,

$$\sigma(\omega) = 2 \tanh \frac{\beta\omega}{2} \int_0^\infty \sin(\omega t) D(t), \quad (3)$$

relating the optical conductivity per particle to the diffusivity. Taking the second derivative yields

$$\frac{d^2\sigma}{d\omega^2} \Big|_{\omega=0} = -\beta \left[2 \int_0^\infty [D - D(t)] t dt + \frac{\mathcal{D}\beta^2}{12} \right]. \quad (4)$$

It is clear from the above relationship that whenever the diffusivity is a monotonically increasing function of time, so that $D(t) < \mathcal{D}$, the curvature is necessarily negative and the optical conductivity will be peaked at $\omega = 0$. This is the case in particular for the band diffusivity shown in Figs. 1c and d, in agreement with the resulting Lorentzian behavior. A necessary condition for the emergence of a finite-frequency peak is instead the existence of a region where $D(t) > \mathcal{D}$, as indeed happens in the transient localization regime as long as $\tau_{in} > t_{loc}$ (orange dashed and red full lines). The present argument therefore reveals a close equivalence between the emergence of a dip in the optical absorption and the crossover condition $\tau_{in} \sim t_{loc}$ stated in the preceding paragraphs.

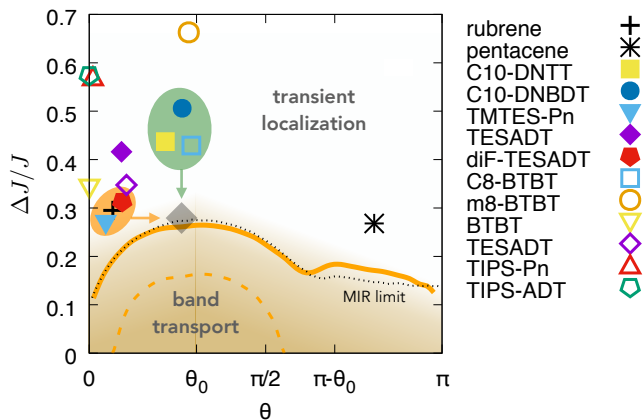


FIG. 3: Phase diagram of room temperature charge transport in organic semiconductors (see text), obtained using $J = 0.1\text{eV}$, $p = 0.05J$ and $T = 0.25J$. Full and dashed line are calculated respectively in the absence of diagonal disorder and with $\Delta = 0.4J$. The dotted line is the MIR limit defined by $(\hbar/\tau)/J = 0.15$. Data points are from Refs. [12] (full symbols) and [14] (open symbols).

The locus of the crossover as determined from the condition $d^2\sigma/d\omega^2|_{\omega=0} = 0$ is reported in Fig. 3 as a function

of the electronic structure parameter θ , providing us with a charge transport "phase diagram" of two-dimensional organic semiconductors (orange full line). The symbols locate the electronic structures and disorder levels calculated for a number of high-mobility organic semiconductors of current interest [12, 14]. For completeness we have included materials that either exactly fulfill the condition $J_b = J_c$, or are sufficiently close to it. Strikingly, all the reported compounds lie within the transient localization regime. In the case of rubrene, in particular, this is in agreement with the fact that a finite-frequency peak has been repeatedly observed in optical absorption experiments [27–29], unequivocally locating this material on the TL side of the crossover.

We note that the crossover line reported here was determined in the ideal situation where the only source of randomness is from transfer integral fluctuations. In real conditions, local site-energy fluctuations originating from the coupling to intra-molecular vibrations as well as extrinsic sources of disorder would shift the crossover to even lower values of $\Delta J/J$, hence pushing the materials deeper into the TL regime. The crossover line calculated in the presence of local gaussian fluctuations of amplitude $\Delta/J = 0.4$ (dashed line) shows that the band regime in that case shrinks down to a very narrow region in the phase diagram. The band regime is totally suppressed at $\Delta/J = 0.5$ (not shown).

Concluding remarks. One may ask if the crossover between the TL and band regime, determined from our microscopic analysis of the electrodynamics of charge carriers, coincides with the breakdown of band theory as inferred from the phenomenological Mott-Ioffe-Regel (MIR) criterion. In one of its formulations, the latter is defined as the point where the semiclassical scattering rate $1/\tau$ reaches values of the order of a fraction of the bandwidth [11, 30, 31]. The MIR condition $(\hbar/\tau)/J = \text{const.}$, with the constant adjusted to 0.15, is shown in Fig. 3 (dotted line). It essentially matches with the crossover line determined above, indicating that in organic semiconductors the breakdown of band theory is closely related with the onset of localization corrections.

As a final remark, the data points in Fig. 3 indicate that while low levels of disorder and isotropic band structures have been independently achieved in current materials (orange and green shaded areas respectively), no compound exists yet that is able to combine such optimal features together. If such a compound could be synthesized, we argue that it should come very close to the semiclassical crossover (arrows and gray diamond), enabling carrier mobilities surpassing those of the current top performers. By combining a relative disorder $\Delta J/J = 0.3$ comparable to that of rubrene, with an optimal, isotropic, set of transfer integrals in the molecular plane, we predict that mobilities around $50 \text{ cm}^2/\text{Vs}$ are in principle within reach, as can be read from Fig. 1a.

S.F. acknowledges support by DFG (Grant No.

DR228/48-1).

-
- [1] H. H. Choi *et al.*, *Nat. Mater.* **17** 2 (2018).
- [2] V. Podzorov *et al.*, *Phys. Rev. Lett.* **93** (8), 086602 (2004).
- [3] W. Xie *et al.*, *J. Phys. Chem. C* **117** (22), 11522 (2013).
- [4] N. A. Minder *et al.*, *Adv. Mater.* **24**, 503 (2012).
- [5] T. Okamoto *et al.*, *Adv. Mater.* **25**, 6392 (2013).
- [6] R. Hofmockel *et al.*, *Organ. Elect.* **12**, 3213 (2013).
- [7] C. Mitsui *et al.*, *Adv. Mater.* **26**, 4546 (2014).
- [8] Y. Krupskaya *et al.*, *Adv. Mater.* **27**, 2453 (2015).
- [9] M. R. Niazi *et al.*, *Nat. Commun.* **6**, 8598 (2015).
- [10] S. Illig *et al.*, *Nat. Commun.* **7**, 10736 (2016).
- [11] S. Fratini, D. Mayou, S. Ciuchi, *Adv. Funct. Mater.* **26**, 2292, (2016).
- [12] S. Fratini, S. Ciuchi, D. Mayou, G. Trambly De Laisardière, A. Troisi, *Nat. Mater.* **16**, 998 (2017).
- [13] T. Kubo *et al.* *Nat. Commun.* **7**, 11156 (2016).
- [14] T. F. Harrelson *et al.* *Mater. Horiz.* **6**, 182 (2019).
- [15] S. Ciuchi, S. Fratini and D. Mayou, *Phys. Rev. B* **83**, 081202(R) (2011).
- [16] S. Ciuchi and S. Fratini, *Phys. Rev. B* **86**, 245201 (2012).
- [17] P. Lee, T. V. Ramakrishnan, *Rev. Mod. Phys.* **57**, 287 (1985).
- [18] N. F. Mott and M. Kaveh, *Adv. Phys.* **34**, 329 (1985).
- [19] P. B. Allen in *Contemporary Concepts of Condensed Matter Science* **2**, 165 (2006).
- [20] D. Mayou, *Phys. Rev. Lett.* **85**, 1290 (2000).
- [21] T. Nematirram, S. Ciuchi, X. Xie, S. Fratini and A. Troisi, *J. Phys. Chem. C*, doi:10.1021/acs.jpcc.8b11916 (2019).
- [22] S. Fratini, S. Ciuchi, D. Mayou, *Phys. Rev. B.* **89**, 235201 (2014).
- [23] The band mobility reported in Fig. 3b of Ref. 12 was mistakenly multiplied by a factor of 2, erroneously resulting in lower μ/μ_{band} ratios.
- [24] G. De Filippis, V. Cataudella, S. Mishchenko, A. N. Nagaosa, A. Fierro, A. de Candia, *Phys. Rev. Lett.* **114**, 086601 (2015).
- [25] M. Kaveh and N. F. Mott, *J. Phys.* **C 15**, L707L716 (1982).
- [26] N. V. Smith, *Phys. Rev. B* **64**, 155106 (2001).
- [27] M. Fischer, M. Dressel, B. Gompf, A.K. Tripathi, and J. Pflaum, *Appl. Phys. Lett.* **89**, 182103 (2006).
- [28] Z. Q. Li, V. Podzorov, N. Sai, M. C. Martin, M. E. Gershenson, M. Di Ventra, and D. N. Basov, *Phys. Rev. Lett.* **99**, 016403 (2007).
- [29] R. Uchida, H. Yada, M. Makino, Y. Matsui, K. Miwa, T. Uemura, J. Takeya, and H. Okamoto, *Appl. Phys. Lett.* **102**, 093301 (2013).
- [30] M. Calandra and O. Gunnarsson, *Phys. Rev. B* **66**, 205105 (2002).
- [31] N. Hussey, K. Takenaka and H. Takagi, *Philos. Mag.* **84**, 2847 (2004).